energies

MDPI

Article

Empirical Validation of a Thermal Model of a Complex Roof Including Phase Change Materials

Stéphane Guichard [1,*], Frédéric Miranville [2], Dimitri Bigot [2], Bruno Malet-Damour [2], Teddy Libelle [2] and Harry Boyer [2]

Received: 9 November 2015; Accepted: 17 December 2015; Published: 24 December 2015
Academic Editor: Chi-Ming Lai

[1] Research Institute in Innovation and Business Sciences (IRISE) Laboratory/Superior Industrial Center Study (CESI)-Reunion Chamber of Commerce and Industry (CCIR)/Regional Centre for the Innovation and Transfer of Technologies (CRITT), The CESI engineering school, Campus Pro—CCIR 65 rue du Père Lafosse-Boîte n°4, Saint-Pierre 97410, France

[2] Physics and Mathematical Engineering Laboratory for Energy, Environment and Building (PIMENT), University of Reunion, 117, rue du Général Ailleret Le Tampon 97430, France; frederic.miranville@univ-reunion.fr (F.M.); dimitri.bigot@univ-reunion.fr (D.B.); bruno.malet-damour@univ-reunion.fr (B.M.-D.); teddy.libelle@me.com (T.L.); harry.boyer@univ-reunion.fr (H.B.)

* Correspondence: sguichard@cesi.fr; Tel.: +262-0262-700-734

Abstract: This paper deals with the empirical validation of a building thermal model of a complex roof including a phase change material (PCM). A mathematical model dedicated to PCMs based on the heat apparent capacity method was implemented in a multi-zone building simulation code, the aim being to increase the understanding of the thermal behavior of the whole building with PCM technologies. In order to empirically validate the model, the methodology is based both on numerical and experimental studies. A parametric sensitivity analysis was performed and a set of parameters of the thermal model has been identified for optimization. The use of the generic optimization program called GenOpt® coupled to the building simulation code enabled to determine the set of adequate parameters. We first present the empirical validation methodology and main results of previous work. We then give an overview of GenOpt® and its coupling with the building simulation code. Finally, once the optimization results are obtained, comparisons of the thermal predictions with measurements are found to be acceptable and are presented.

Keywords: phase change materials (PCMs); building thermal simulation; model optimization; model validation

1. Introduction

Buildings are indisputably considered as one of the largest energy consuming sectors. According to the International Energy Agency (IEA), the average energy consumed by buildings represents 32% of worldwide energy consumption, with approximately 40% of the primary energy used in most countries. In France, the energetic consumption in the building sector is approximately about 43%, representing a quarter of the nation's carbon dioxide emissions. The use of energy-hungry appliances to improve the thermal comfort is responsible for both the electrical energy consumption and the increase of greenhouse gas emissions [1].

For this reason, some actions are performed to curb energy consumption and to protect the environment, for example, the use of renewable energies, passive energy buildings and the use of appropriate building codes for new or retrofitted buildings. Moreover, several studies and applications have shown that the building thermal inertia is among the possible solutions and should

be improved, in order to achieve high performance and low-energy buildings [2–4]. As a result, the question of the increase of the thermal energy capacity storage of materials used in the building sector arises. With this target in mind, a technology such as the use of phase change materials (PCMs) may be integrated into building envelopes, both to enhance the thermal energy storage [5] and to improve the thermal comfort. Indeed, because of their higher thermal energy storage densities than other heat storage materials, these materials are able to store and release thermal energy as latent heat, when the phase change occurs. It is important to highlight the fact that the latent heat storage is much larger than the sensible heat storage [6]. Usually, organic and inorganic PCMs are often used and solid-liquid phases are chosen [7]. Despite the fact its thermal conductivity should be improved, paraffin is often used for latent heat thermal energy storage [8]. Indeed, it has useful thermal properties such as absence of supercooling, chemical stability and a low vapor pressure [3,9].

The use of PCMs in the building envelope may reduce the peak loads due to heating, ventilating and air conditioning (HVAC) energy consumptions by increasing the thermal inertia of each wall of the building. The peak load may thus be shifted to the off-peak energy use load periods [10]. In addition, the results of PCM-oriented research on buildings have shown that the thermal comfort was improved and energy savings could be achieved.

Among all the PCM applications to achieve high energy efficiency buildings, for example PCM-integrated walls, PCM-assisted ceiling heating and cooling, photovoltaic systems coupled with a PCM-based heat storage system [11], and so on, this paper deals with the inclusion of PCMs in the roof system. Generally, the roof is considered as a thermal buffer between the indoor and outdoor environment. This is the part of the building most exposed to solar radiation in hot climates and considered as the weakest part of a building's thermal performance [12,13].

One possible solution to reduce heat transfer from outside to inside a building may be found in the increased use of mass insulation. Nevertheless, this type of thermal insulation allows one to reduce heat transfer due to conduction, but does not reduce heat transfer by infrared radiation through the roofing. To overcome this drawback, a solution based on the use of radiant barrier systems, which requires the presence of air layers in order to minimize radiation heat transfer, is proposed [12]. Based on the same approach, PCM under a flexible sheet form laminated on both sides with an aluminum sheet is used in the lower part of the roof between the air layer and the drywall, both to enhance the thermal energy storage and to reduce the solar radiation through the roof system [14]. Furthermore, before integrating PCM into new or retrofitted buildings, it is interesting to predict the thermal effects of these materials on the whole building performance. To contribute to the energy efficiency policy recommendations for buildings' energy consumption, a one-dimensional simplified numerical model for PCMs has been developed and implemented in a prototype building simulation code named ISOLAB. ISOLAB is able to take into account the building envelopes, including PCM or not, and their actual impacts on energy consumption. Nevertheless, before using the PCMs model integrated in the ISOLAB code and to ensure the reliability of the results, this article focuses on the empirically validation of the latter. We first present the tools used, building simulation code and the generic optimization program GenOpt®. We then briefly describe the studied system as well as the main results of previous work. Finally, results of the experimental validation of the thermal model are presented and discussed.

2. Presentation of Tools

2.1. A Building Simulation Code: ISOLAB

Developed by Miranville [15], ISOLAB is a prototype building simulation software developed with the Matlab environment. Nodal descriptions of buildings and a finite difference scheme of the time variable in one-dimension are used to simulate the dynamic thermal behavior of a monozone or multi-zone building according to its environment (weather data and location). In order to determine

temperatures of the whole building, the following matrix formalism Equation (1) is solved by using an implicit finite-difference method [16]:

$$C_w \dot{T}_w = A_w T_w + B_w \quad (1)$$

where the index w is used for walls and windows. A_w is the state matrix including the terms linked to heat conduction and the interior linearized convective exchanges. B_w is the vector containing outside or internal solicitations of the system. C_w is the capacities matrix. T_w is the state vector containing every temperature of each wall and $\dot{T}_w$ is the temperature derivative of T_w. The ISOLAB code has already been validated with the International Energy Agency, Building Energy Simulation Test (IEA BESTEST) procedure, concerned with buildings without PCMs [15].

2.2. A Generic Optimization Program: GenOpt®

The optimization process consists in running several model simulations with different parameters sets. The chosen parameters are identified by using a mathematical tool like parametric sensitivity analysis. Thereafter, each simulation is launched with a different set of parameters (continuous parameters, discrete parameters, or both), and the associated cost function value, with or without constraints, is recorded. Finally, to ensure convergence to the best set of parameters, it is necessary to run many simulations varying each parameter within the right range.

A generic optimization program called GenOpt® from the Lawrence Berkeley National Laboratory of the University of California, developed with the Java environment by Wetter, is used to optimize the unknown parameters [17]. The choice of GenOpt® has been made according to its simulation program interface that allows the coupling with any simulation program, without requiring code modifications. Indeed, the coupling is done by creating files required by GenOpt® to run an optimization and also an auto-executable version of the model [18]. In addition, GenOpt® is dedicated for the thermal building simulation. For more details about the generic optimization program, the interested reader may refer to [17]. Before performing the optimization sequences with GenOpt®, the studied system with the main results of previous work are presented in the following section.

3. Experimental Set up of a Complex Standard Roof Including Phase Change Materials

3.1. Introduction

The objective of this part is to show the main results of experimental investigations on a complex roof incorporating PCM panels. The use of such a database allows us to empirically validate the numerical code developed and implemented in a prototype building simulation software to determinate the thermal performance of any building envelopes with PCM. First, a description of the roofing complex and the associated instrumentation is presented below.

3.2. Localization and Structure of the Test Cell

With dimensions of 3 m (height) × 3 m (width) × 3 m (length) and an internal volume about 30 m^3, the test cell, called industrial engineering laboratory (LGI), can be considered a typical room of existing buildings on Reunion Island. It has been designed with a flexible structure in order to study several configurations and phenomena. Thanks to its modular structure, the movable walls allow testing PCM panels included in the standard roof inclined 20° with respect to the horizontal. The whole building envelope is constituted of vertical opaque walls, a jalousie type window, a glass door and a complex roof with PCM panels. The roofing complex is an assembly of homogeneous or inhomogeneous materials, separated by one or several air layers [12,14,18]. The building components of LGI are given in Table 1, and an overview is depicted in Figure 1a. In steady

state conditions and applying the French thermal rules [19], the U-value of each wall is calculated using the following formula:

$$\frac{1}{U} = \frac{1}{h_{ext}} + \sum_{i=1}^{n} \frac{e_i}{\lambda_i} + \frac{1}{h_{in}}, \quad (2)$$

with $h_{ext} = h_{re} + h_{ce}$ and $h_{in} = h_{ri} + h_{ci}$. The U-values of the construction are also given in Table 1.

Table 1. Arrangement of the LGI test cell [13]. Phase change material: PCM.

Element	Composition	Remark (s)
Opaque vertical walls	Sandwich board 80 mm thick cement-fiber/polyurethane/cement-fiber	U_{walls} = 0.4 W·m^{-2}·K^{-1}
Window	Aluminium frame, 8 mm clear glass	Blind-type 0.8 m × 0.8 m
Glass door	Aluminium frame, 8 mm clear glass	Glass in upper and lower parts, 0.7 m × 2.2 m
Roofing complex	Corrugated galvanised steel 1 mm/air layer of 280 mm thick/PCM 5.26 mm thick/Plasterboard 12.5 mm	PCM is laminated to aluminium protective foils. Roof inclined at 20°. U_{roof} = 2 W·m^{-2}·K^{-1}
Floor	Concrete slabs 80 mm thick on 60 mm thick polystyrene	U_{floor} = 0.7 W·m^{-2}·K^{-1}

(**a**) (**b**)

Figure 1. (**a**) Industrial engineering laboratory (LGI) cell; and (**b**) experimental platform.

Located at a low altitude (68 m) above sea level, the experimental set-up was erected on the experimental platform of the University Institute of Technology of Saint-Pierre (Reunion Island). This choice of location implies the study of a tropical climate with strong solar radiation and humidity. Besides, the test cell is oriented north in order to receive symmetrical solar radiation during the day [14]. To obtain extreme solicitations inputs from the roof, a dark blue color has been chosen for the corrugated iron. During the experimental validation procedure, the blind windows and the window panes were masked, and the test cell was kept closed, without using mechanical ventilation or an air-conditioning system [13].

Furthermore, near the experimental devices, two meteorological stations (the weather station is depicted in a red circle in Figure 1b) are installed in order to collect data from the environment, such as solar radiation (global, direct and diffuse, on a horizontal plane), ambient air temperature, exterior relativity humidity, wind speed and direction. As depicted in Figures 2 and 3 and because of the significant duration of the chosen experimental sequence (approximately 92 days), only five days of data from August to October 2012 are presented in this paper.

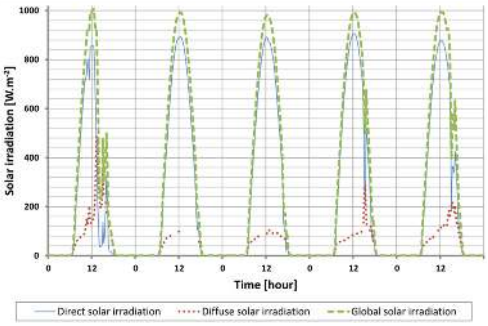

Figure 2. Solar irradiation from 20 to 24 September 2012 [13].

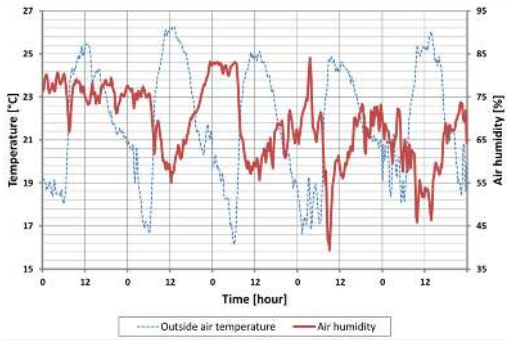

Figure 3. Outside air temperature and air humidity from 20 to 24 September 2012 [13].

3.2.1. Instrumentation of the Enclosure

Sixty sensors located both in the enclosure and on the roof of the LGI test cell have been used. The walls (north, south, east and west, inside and outside) are equipped with thermal sensors on the surfaces, such as T-type thermocouples and flux meters in order to measure the inside or outside surface temperature of each wall. For air temperature, the thermocouples are inserted into aluminum cylinders. For radiant temperature, the thermocouples are contained in a black globe.

To assess the stratification of the air, the interior volume was measured at three different heights from floor to ceiling (Figure 4). Many heat sensors have been sealed in the concrete slabs supporting the cell, in order to assess the information on the boundary conditions from the ground. Indeed, modeling errors concerning this part of the building, the ground measurements database is used during the code validation step. For more details on sensors' locations and set-up and the on the associated errors, the interested reader may refer to [13].

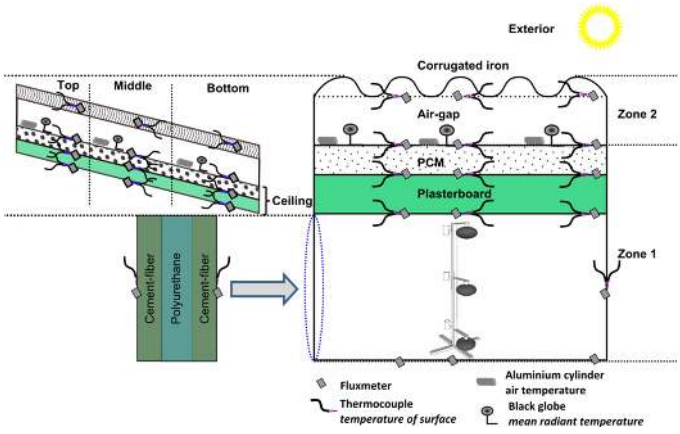

Figure 4. Simplified schematic of the LGI cell and instrumentation.

3.2.2. Instrumentation of the Roof

To ensure reliable measurements of the complex roof, sensors have been located as depicted in Figure 4. To assess temperatures and heat flux measurements from the corrugated iron to the ceiling, each component of the complex roof was instrumented. The heat sensors are spread on both sides of the surfaces of the corrugated iron, on the PCM panels and on the drywall. Between the PCM panels and the corrugated iron, the air layer is not ventilated, and the dry-air and black globe temperatures were also measured.

Before using the heat sensors, the thermocouples were calibrated and verified on site according to a convenient procedure. Heat flux sensors were calibrated by the manufacturer. The accuracy of the thermocouples is estimated to ± 0.5 °C, and according to manufacturer, the relative error of flux meters is approximately about 5%. In order to avoid air bubbles for both thermocouples and flux meters, thus causing thermal resistances of contact, a conductive heat paste was applied on the surfaces. A data logger was installed in the LGI cell in order to collect data from all the sensors every 15 min. All data were saved on a computer [13].

4. Previous Investigation

4.1. Introduction

Before May 2013, both the thermal behavior of building envelopes including PCM and time-varying thermal properties of materials were not taken into account by ISOLAB. For this, a simplified numerical model of the thermal behavior of PCMs was developed and implemented. However, many constraints on the PCM model have been imposed, such as the respect of the state system formalism and the use of an implicit one-dimensional scheme according to the finite difference approach. Moreover, the apparent heat capacity method has been used.

4.2. Description of the Roofing Complex

The model is intended to predict temperature evolutions of each components of the whole building, including the inside air of enclosures. The studied LGI cell is considered as well-isolated and divided into two thermal zones. The ceiling is a specific wall separating the two vertical zones. It plays the role of ceiling for the first zone and of floor for the second zone. We note that the air gap simulated in zone 2 is considered as a thermal zone in our multi-zone building model (Figure 4).

The presence of an air layer between the corrugated iron and PCM panels allows one to benefit from the principle of action of reflective insulation, which is closely linked to the radiative properties of the surfaces of PCM panels. Taking into account the air layer with the combination of homogenous and inhomogeneous materials, the roof system can be qualified as complex with coupled heat transfers involved (conduction, convection and radiative transfers) [20]. Therefore, the chosen configuration may complicate the determination of thermal performances due to the multiple configurations of the air layer: opened or closed, naturally ventilated or forced-ventilated [14]. This is the reason that explains why the enclosed air space is considered as a thermal zone in the approach proposed in this paper.

4.3. Description of Phase Change Material Test

Tested PCMs are commercial products from Dupont™ Energain®. They consist of 5 mm thick flexible sheets, made of 60% microencapsulated paraffin wax within a copolymer laminated on both sides with an aluminum sheet [13,14]. The panels' characteristics are summarized in Table 2.

Values of the heat capacity in each phase and melting point have been determined by differential scanning calorimetry (DSC) measurements. These parameters are exposed in details in [21,22].

Table 2. Characteristics of PCMs used [13].

Parameters		Value	Unit
Thermal properties	Thermal conductivity: λ_s/λ_l	0.22/0.18	$W\cdot m^{-1}\cdot K^{-1}$
	Heat capacity: C_{ps}/C_{pl}	3134/2833	$J\cdot kg^{-1}\cdot K^{-1}$
	Latent heat: $L_{melting}$	71	$KJ\cdot kg^{-1}$
	Melting temperature	23.4	°C
Descriptive properties	Thickness	5.26	mm
	Width	1000	mm
	Length	1198	mm

4.4. Mathematical Model for Phase Change Material

The solidification and melting process are the most studied in building applications. Usually, numerical modelling of these phenomena is either based on the first or second law of thermodynamics. For more details, the interested reader may refer to [23].

The thermal model for phase change is based on the apparent heat capacity method from the enthalpy method. This method allows one to obtain the general form of a heat conduction equation with a nonlinear specific heat, without needing to know ahead of time the location of the phase interface. To simplify the mathematical model, some assumptions were made [13,14,24]. Through the solid (or liquid) fraction term, called f_s, the final expression of transient heat conduction can be written in 1-D along the $\vec{x}$ direction as follows [13,24]:

$$C_{app}(T)\frac{\partial T(x,t)}{\partial t} = \lambda_{PCM}(T)\frac{\partial^2 T(x,t)}{\partial x^2}$$

$$\text{With: } \begin{cases} C_{app}(T) = \rho_s c_s + \Delta(\rho c) f_s + \dfrac{df_s(T)}{dT}\left(\rho_l L_m + \Delta(\rho c)\cdot\left(T(x,t) - T_m\right)\right) \\ \Delta(\rho c) = \rho_l c_l - \rho_s c_s \\ \lambda_{PCM}(T) = (1 - f_s(T))\lambda_s + \lambda_l f_s(T) \\ f_s(T) = \dfrac{1}{2} - \dfrac{1}{2}\tanh\left(\gamma\dfrac{T_m - T(x,t)}{4\delta T}\right) \\ \dfrac{df_s(T)}{dT} = \dfrac{\gamma}{8\Delta T\left[\cosh\left(\gamma\dfrac{T_m - T(x,t)}{4\delta T}\right)\right]^2} \end{cases} \quad (3)$$

The governing equation in terms of the apparent heat capacity can be solved using a standard heat transfer code, and a wide range of discretization approaches can be used. As a result, the one-dimensional finite difference method can be chosen [20]. To definitely be in accordance with the formalism of the ISOLAB equation, the use of a backward Euler scheme is possible thanks to the solid (or liquid) fraction term. Generally, the expression of the solid fraction is given by using an approximation of the Heaviside function. In the PCM model, a specific parameter called γ appears in the final expression. The latter is usually equal to 1, for instance in [25]. In order to not underestimate or overestimate the latent heat value during the phase change process, a proposed method was given by [13]. For a given phase change interval δT, and at $T = T_m$, the expression of the apparent heat capacity (C_{app}) leads to the first determination of γ, according to the following process [13]:

If $T(x,t) \geqslant T_m - \delta T$ *and* $T(x,t) \leqslant T_m + \delta T$ then :

$$\left|\max(\gamma) = \left(\max(C_{DSC}) - \left(\frac{c_s + c_l}{2}\right)\right)\cdot\frac{8\delta T}{L_m}\right.$$

else

$|\gamma$ must be determined

end

where $\max(C_{DSC})$ is given by DSC, and δT is chosen very small. In the numerical simulation, $\delta T = 0.01$C. In the first approach, γ is evaluated as follows:

$$\gamma = \frac{L_m}{C_{ps} \cdot (T_m - \delta T)} \quad (4)$$

It is important to highlight that the model of the test cell with PCMs takes into account all heat transfer modes (radiative heat transfer, convection heat transfer and conduction heat transfer), the related values being presented in detail in [13]. Besides, the radiative model is based on specific developments for low emissivity walls and thus includes the effects of the reflective surfaces of the PCM panels [26].

4.5. Main Results

The thermal model is considered validated only if the validation criteria are met. These criteria are given by [13,18]:

(1) To reach 10% validation error between numerical solutions and experimental data from actual building;
(2) To reach acceptable absolute errors between some numerical solutions and measurements:

- $\pm$ 2 °C for temperatures on each side of each suspended ceiling
- $\pm$ 1 °C for indoor air temperature of real building

To definitely validate the numerical thermal model, different steps are required. These steps are illustrated in Figure 5: the two first steps have already been presented in details in [13]. The results showed that the numerical thermal model was able to predict the dynamic thermal behavior of PCMs. Nevertheless, the validity criteria were not respected. According to the validation methodology, it was necessary to highlight the origins of errors. A parametric sensitivity analysis, according to a method derived from the fast Fourier amplitude transform (FAST) method has been performed and this made it possible to put in evidence the parameters with most influence on model outputs [27–29]. Following the sensitivity analysis, the main causes of any differences between the model and experimental data can be explained, but also we can focus on the search of the set of unknown parameters of the model in a restricted range. The following important results were shown [13]:

- The thermal behavior of the complex roof is governed by convective heat transfers, both in the air layer and the faces of the suspended ceiling.
- The absorptivity coefficient of corrugated iron was not the same as new sample.
- The specific parameter γ can be considered as a non-dimensional velocity of phase change because the phase change is assumed to occur slowly. This parameter can also be used to overcome numerical instabilities in the zone near the interface between the two phases of the PCM. Indeed, during the phase change, a mushy zone between the two phases is created. From a numerical point of view, sharp discontinuities at the phase interface are observed, implying some very difficult to overcome numerical instabilities. Moreover, it influences the derivative gradient of the solid fraction. However, its physical interpretation is still in investigation.

The parameters linked to the convective exchange coefficients are depicted in Figure 6 and all parameters are given by the Table 3. However, the unknown parameters have to be determined. For this, optimization sequences were performed.

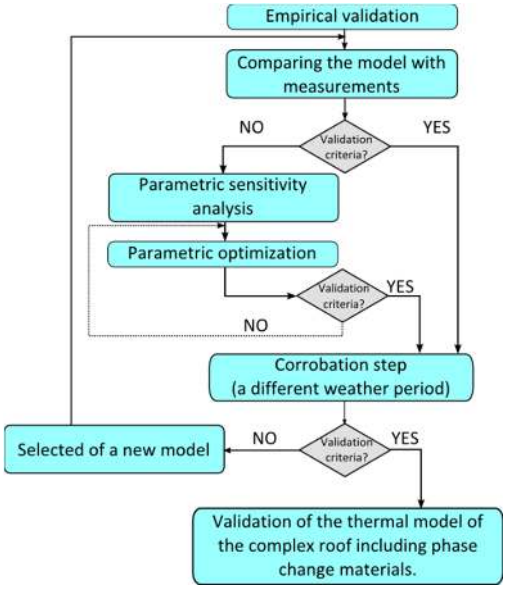

Figure 5. Methodology used for the empirical validation.

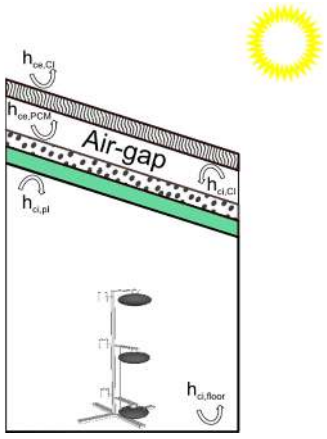

Figure 6. Most influential convective exchange coefficients.

Table 3. Most influential parameters on model outputs at the end of sensitivity analysis step.

Frequency	Parameters	Unit
103 ($h_{ci,floor}$)	Indoor convective exchange coefficient of the floor (zone 1)	$W \cdot m^{-2} \cdot K^{-1}$
107 ($h_{ci,pl}$)	Indoor convective exchange coefficient of the plasterboard	$W \cdot m^{-2} \cdot K^{-1}$
108 ($h$ci,PCM)	Outdoor convective exchange coefficient of the PCM panel	$W \cdot m^{-2} \cdot K^{-1}$
154	γ coefficient	-
199 ($h_{ci,CI}$)	Indoor convective exchange coefficient of the corrugated iron	$W \cdot m^{-2} \cdot K^{-1}$
200 ($h_{ce,CI}$)	Outdoor convective exchange coefficient of the corrugated iron	$W \cdot m^{-2} \cdot K^{-1}$
218 (α_{CI})	Solar absorptivity coefficient of the corrugated iron	-

5. Empirical Validation of the Phase Change Material Model

5.1. Phase Change Material Model Optimization Using GenOpt®

The optimization sequence consists in achieving the best set of parameters by maximizing or minimizing a chosen cost function, subject to a set of constraints (or a defined domain), until

optimization criteria are met. Indeed, many simulations are run and when a stopping criterion is reached, like the required error on the studied output for instance, the optimization is stopped.

To optimize the thermal model of PCM implemented in ISOLAB by using GenOpt®, a methodology for the coupling of the building simulation code with the optimization program is required. The study has already been published and the interested reader may see [18] for details.

Among the various methods of fixing sets of parameters implemented in GenOpt®, the generalized pattern search (GPS) Hooke-Jeeves MultiStart Algorithm was used. Indeed, it allows to look over some parameters and to avoid the result values to be obtained from a local minimum value. In addition, this algorithm is compatible with all building thermal insulation codes and gives reliable results. The cost function used is calculated by using a mathematical model tool based on the modified standard deviation:

$$s = \sqrt{\frac{1}{n}\sum_{i=1}^{n}(x_i - \bar{x})^2} \quad (5)$$

If several model outputs are used to optimize the model, the global cost function is the sum of the absolute values of costs functions for each output. The optimization sequence is stopped, if and only if, same minimum values of the cost functions were reached for 10 different optimization sequences. In our approach, several optimization sequences (1500 optimization sequences were reached approximately) and statistics studies were performed.

5.2. Results of the Optimization

Results from the optimization sequence are summarized in Table 4.

Table 4. Parameters before and after optimization sequences.

Parameters	Before Optimization	After Optimization	Unit
$h_{ci,floor}$	3.50	5.00	$W \cdot m^{-2} \cdot K^{-1}$
$h_{ci,w}$	1.00	1.00	$W \cdot m^{-2} \cdot K^{-1}$
$h_{ci,PCM}$	1.00	1.50	$W \cdot m^{-2} \cdot K^{-1}$
γ (when $T \neq T_m$)	0.04	0.01	-
$h_{ci,CI}$	3.50	1.75	$W \cdot m^{-2} \cdot K^{-1}$
$h_{ce,CI}$	25	5.7 V + 11.4 [15]	$W \cdot m^{-2} \cdot K^{-1}$
α_{CI}	0.85	0.76	-

Each value of an optimized parameter is found in agreement with the physical phenomena. Indeed, convective exchange coefficients are very small and correspond to the non-ventilated upper air layer as the building was kept closed during the experimental sequence. To apply the process for determining the γ parameter, this coefficient has been evaluated to 0.01 when $T \neq T_m$. The value of absorptivity coefficient (α_{CI}) is equal to the value that was determined by [30]. This value, lower than initially expected, can be justified by the fact that the cell was erected and covered a few years ago, time tending to decrease the absorptivity or dark color of the roof. Indeed, over time, the performances of buildings will not be the same than when the building was new [15].

5.3. Comparison between Optimized Thermal Model of Phase Change Material with Measurements

On the whole period, the dynamic behaviour of the components of the complex roof and the indoor air temperature are predicted well. Through the different curves (Figure 7), we can ensure that the given melting temperature for this application was correctly chosen because the temperatures on both sides of PCM allow the storage and the release of energy during phase change process.

The surface temperature of the suspended ceiling is predicted at ± 1.3 °C (Figure 8). The used conditions show that PCM model is able to properly predict the behavior of the PCM panel. The comparison between numerical simulations and experimental data shows a good agreement. The

indoor air temperature of LGI test cell is predicted with an accuracy of ± 0.5 °C (Figure 9). The criteria for the validation of the thermal model are respected. According to Table 5, the mean errors between numerical solutions and experimental measurements do not exceed 5%.

Table 5. Standard deviations, maximum differences and errors after optimization sequences.

Localization	Standard Deviation σ (°C)	Maximum Difference (°C)	Maximum Error (%)	Mean Error (%)
Inside air temperature (zone 1)	0.2	− 0.5	− 6.2	2.1
Suspended ceiling inside surface temperature (plasterboard)	0.4	− 1.1	− 8.9	2.9
Interface PCM/plasterboard temperature	0.4	− 1.3	8.8	3.1
Suspending ceiling outside surface temperature (PCM)	0.5	− 1.7	− 9.8	2.3
Air-gap temperature (zone 2)	1.0	− 2.6	− 9.4	3.1
Corrugated iron temperature	1.3	3.5	9.4	3.2

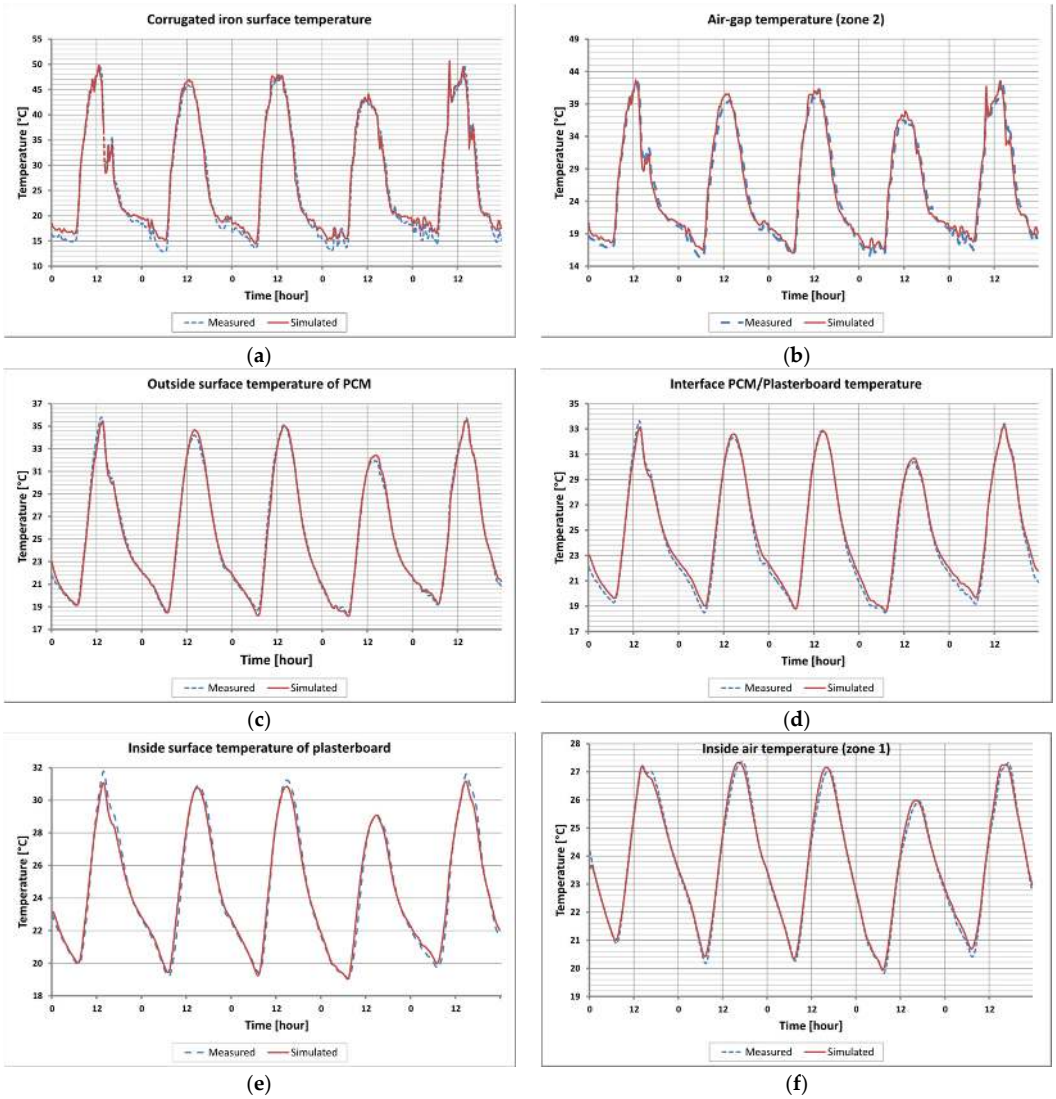

Figure 7. Comparison of model results with experimental measurements for all components of the complex roof (**a**–**e**) and for inside air temperature (**f**) (zone 1).

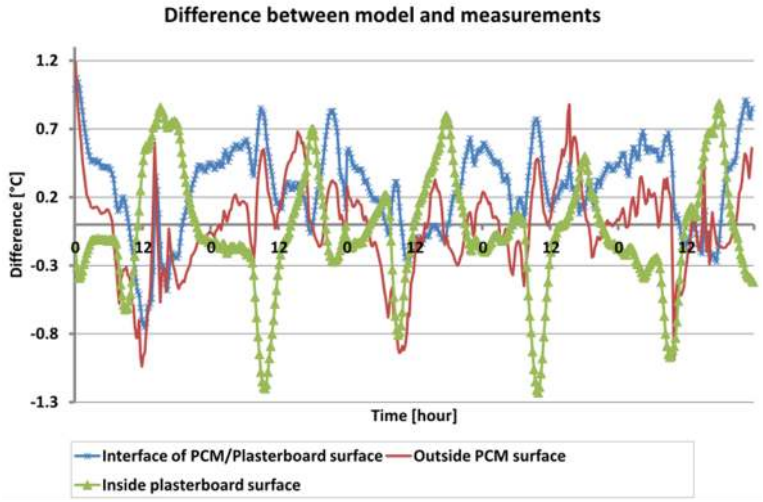

Figure 8. Errors between numerical solutions and experimental data for suspended ceiling temperatures.

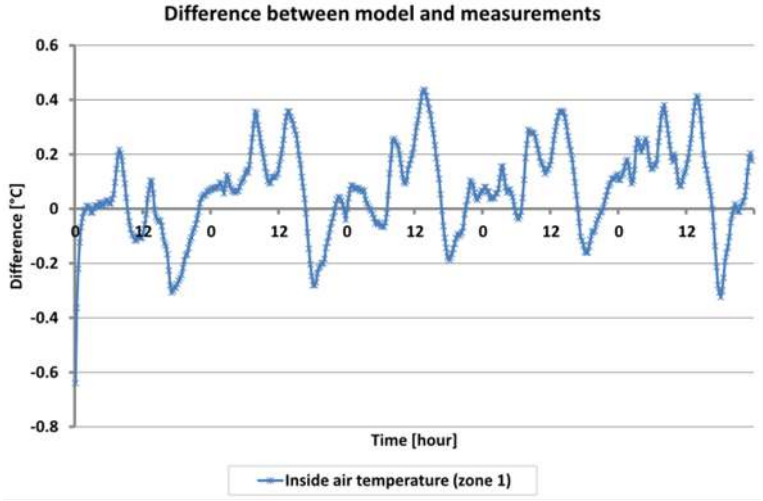

Figure 9. Errors between numerical solutions and experimental data for inside air temperature.

The most important errors result from the prediction of the air-gap temperature and the prediction of the metal sheet temperature in zone 2. For the air-gap, the model must be improved and models from the literature based on computational fluid dynamics (CFD) showed that the results are inconclusive due to the influence of boundary conditions. Thus, an empirical correlation from experiments will have to be determined. Nevertheless, the values of convective exchange coefficients ($h_{ce,CI}$ and $h_{ci,PCM}$) determined by the optimization sequences correspond with the empirical correlation developed by Alamdari and Hammond [31] (it has been verified later that the obtained results fit the correlation). The proposal of these authors is a combination of two correlations for taking into account both natural convection in laminar regime and turbulent regime:

$$h = \left[\left(1.51 \frac{|\Delta T|^{\frac{1}{4}}}{H} \right)^6 + \left(1.33 \, |\Delta T|^{\frac{1}{3}} \right)^6 \right]^{\frac{1}{6}} \quad (5)$$

where ΔT is the averaged difference temperature between the surface of the wall and the indoor air of the room. H corresponds to the height of the wall.

With the predicted air temperature in zone 2, the errors between the curves can also be explained by the prediction of the corrugated iron surface temperature. Indeed, the latter has a direct effect on the temperature of each component of the complex roof. To reduce these errors, the radiative model should be improved and the radiosity method should be used [15].

To conclude this step, the thermal model was fully-coupled with the ISOLAB code and the results of the PCM model are very encouraging. Indeed, for different type of walls with PCM or not, the model is able to predict temperatures in actual conditions. However, to definitely validate the PCM model implemented in the ISOLAB building simulation code, it is necessary to compare numerical solutions with another experimental data sequence as presented in the next part.

5.4. The Corroboration Step

The corroboration step consists in using another experimental period in order to verify if all parameters determined can be generalized and are not specific for a given period. Moreover, it also allows evaluating the efficiency of the proposed model. For this step of corroboration, the meteorological data used are from 2 to 5 October 2012. This period was characterized by [20]:

- an average maximal global radiation of 900 $W \cdot m^{-2}$
- an average wind speed of 3.50 $m \cdot s^{-1}$
- an average outdoor temperature of 26 °C
- an average rate humidity of 65%

The results from the corroboration step are summarized in Table 6. In this part, the validation criteria are also respected. For instance, comparison between numerical simulations and measurements for the predicted indoor air temperature is depicted in Figure 10. For more details, the interested reader may refer to [20].

Table 6. Standard deviations, maximum differences and errors for the corroboration period.

Localization	Standard Deviation σ (°C)	Maximum Difference (°C)	Maximum Error (%)	Mean Error (%)
Inside air temperature (zone 1)	0.2	0.6	5.6	2.1
Suspended ceiling inside surface temperature (plasterboard)	0.5	1.5	9.2	3.4
Interface PCM/plasterboard temperature	0.5	1.7	8.9	3.6
Suspending ceiling outside surface temperature (PCM)	0.5	1.7	9.9	2.8
Air-gap temperature (zone 2)	1.3	3.4	8.9	3.2
Corrugated iron temperature	1.6	4.7	9.8	3.3

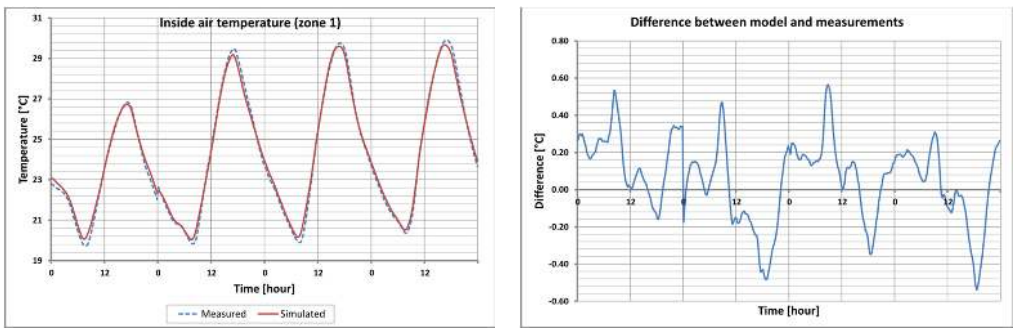

(**a**) (**b**)

Figure 10. Comparison (**a**) and errors (**b**) between model results with experimental measurements for inside air temperature (zone 1) during the corroboration step.

Tables 5 and 6 show that maximum differences between predictions and measurements are a little more important than the results of the first experimental sequence. A possible explanation is a high setting of parameters for specific environmental conditions. Nevertheless, despite these differences the model can be considered as valid because the validation criteria have again been reached. Furthermore, the maximal standard deviation is approximately of 1.6 °C and all mean errors are below 5%.

6. Conclusions and Further Works

In this paper, a generic thermal model of PCM in buildings, validated with reliable experimental data, was presented. An actual building equipped with PCM in a complex roof was set up and each component's surfaces in contact with the indoor air temperature were measured. A detailed investigation was carried out to evaluate the efficiency of the thermal behavior of the model, with important steps included in experimental validation.

A mathematical model based on the apparent heat capacity has been presented. Moreover, an approach of nodal description of the complex wall and a finite difference method in one-dimensional were used. Thanks to parametric sensitivity analysis, the most influential factors on model outputs such as, all convective exchange coefficients, γ parameter and the absorptivity coefficient of corrugated iron, were determined by a generic optimization tool. Then, a new comparison between the optimized thermal model and experimental data was performed. With the corroboration step, the results showed that the validity criteria were respected. Finally, the validation process of model has been reached and the thermal model of PCM has been validated.

Despite the empirical validity of the PCM model, further work is necessary to improve the air-gap temperature prediction and the radiative model used in order to obtain better agreement between the numerical solutions and measurements. Moreover, a mathematical formulation of the γ parameter should be presented. Other experimental studies should be performed to confirm the use of these materials in tropical climates such as Reunion Island. Future works will also focus on the comfort study from the dedicated test cell.

Acknowledgments: The authors wish to thank Fonds Social Européen and La Région Réunion for their support and their fundings of the first author's thesis. In addition, this research received funding from the Ministère de l'Outre-Mer.

Author Contributions: Stéphane Guichard designed the experiments and developed PCM model for the experimental and numerical studies. Frédéric Miranville, Dimitri Bigot and Harry Boyer helped for the coupling model of PCM with ISOLAB code and performed the validation stages of this one. Bruno Malet-Damour and Teddy Libelle helped to monitor the data from the experimentation in order to ensure they were reliable for the empirical validation of the PCM model.

Conflicts of Interest: The authors declare no conflict of interest.

Nomenclature

Variables

c	Specific capacity ($J \cdot kg^{-1} \cdot K^{-1}$)
C	Apparent heat capacity ($J \cdot m^{-3} \cdot K^{-1}$)
f	Solid or liquid fraction
h	Convection heat transfer coefficient ($W \cdot m^{-2} \cdot K^{-1}$)
L	Latent heat ($J \cdot kg^{-1}$)
T	Temperature (°C)
t	Time (s)
x	Spatial variable (m)
U	Thermal conductance ($W \cdot m^{-2} \cdot K^{-1}$)
V	Wind speed ($m \cdot s^{-1}$)

Subscripts

ce	Exterior convection
ci	Interior convection
ext	Exterior
int	Interior
l	Liquid phase
m	Melting point
re	Exterior radiative
ri	Interior radiative
s	Solid phase

Greek Symbols

γ	Constant parameter
δT	Phase change interval (°C)
ρ	Density ($kg \cdot m^{-3}$)
λ	Thermal conductivity ($W \cdot m^{-1} \cdot K^{-1}$)

Abbreviations

IEA BESTEST	International Energy Agency, Building Energy Simulation Test
ISOLAB	A building simulation software, which integrates the hygro-thermal and aeraulic phenomena
PCM	Phase change material

References

1. Pérez-Lombard, L.; Ortiz, J.; Pout, C. A review on buildings energy consumption information. *Energy Build.* **2008**, *40*, 394–398. [CrossRef]
2. Zhou, D.; Zhao, C.-Y.; Tian, Y. Review on thermal energy storage with phase change materials (PCMs) in building applications. *Appl. Energy* **2012**, *92*, 593–605. [CrossRef]
3. Zalba, B.; Marín, J.M.; Cabeza, L.F.; Mehling, H. Review on thermal energy storage with phase change: Materials, heat transfer analysis and applications. *Appl. Therm. Eng.* **2003**, *23*, 251–283. [CrossRef]
4. Farid, M.M.; Khudhair, A.M.; Razack, S.A.K.; Al-Hallaj, S. A review on phase change energy storage: Materials and applications. *Energy Convers. Manag.* **2004**, *45*, 1597–1615. [CrossRef]
5. Cabeza, L.F.; Castell, A.; Barreneche, C.; de Gracia, A.; Fernández, A.I. Materials used as PCM in thermal energy storage in buildings: A review. *Renew. Sustain. Energy Rev.* **2011**, *15*, 1675–1695. [CrossRef]
6. Seong, Y.-B.; Lim, J.-H. Energy Saving Potentials of Phase Change Materials Applied to Lightweight Building Envelopes. *Energies* **2013**, *6*, 5219–5230. [CrossRef]
7. Hasan, A.; McCormack, S.J.; Huang, M.J.; Norton, B. Energy and cost saving of a photovoltaic-phase change materials (PV-PCM) system through temperature regulation and performance enhancement of photovoltaics. *Energies* **2014**, *7*, 1318–1331. [CrossRef]
8. Medina, M.A.; King, J.B.; Zhang, M. On the heat transfer rate reduction of structural insulated panels (SIPs) outfitted with phase change materials (PCMs). *Energy* **2008**, *33*, 667–678. [CrossRef]
9. Sarı, A.; Karaipekli, A. Thermal conductivity and latent heat thermal energy storage characteristics of paraffin/expanded graphite composite as phase change material. *Appl. Therm. Eng.* **2007**, *27*, 1271–1277. [CrossRef]
10. Khudhair, A.M.; Farid, M.M. A review on energy conservation in building applications with thermal storage by latent heat using phase change materials. *Energy Convers. Manag.* **2004**, *45*, 263–275. [CrossRef]
11. Lo Brano, V.; Ciulla, G.; Piacentino, A.; Cardona, F. On the efficacy of PCM to shave peak temperature of crystalline photovoltaic panels: An FDM model and field validation. *Energies* **2013**, *6*, 6188–6210. [CrossRef]
12. Miranville, F.; Boyer, H.; Lauret, P.; Lucas, F. A combined approach for determining the thermal performance of radiant barriers under field conditions. *Solar Energy* **2008**, *82*, 399–410. [CrossRef]

13. Guichard, S.; Miranville, F.; Bigot, D.; Boyer, H. A thermal model for phase change materials in a building roof for a tropical and humid climate: Model description and elements of validation. *Energy Build.* **2014**, *70*, 71–80. [CrossRef]
14. Guichard, S.; Miranville, F.; Bigot, D.; Malet-Damour, B.; Boyer, H. Experimental investigation on a complex roof incorporating phase-change material. *Energy Build.* **2015**, *108*, 36–43. [CrossRef]
15. Miranville, F. *Contribution à l'étude des parois complexes en physique du bâtiment modélisation, expérimentation et validation expérimentale de complexes de toitures incluant des produits minces réfléchissants en climat tropical humide*; Université de la Réunion: Saint-Pierre, France, 2002. (In French)
16. Boyer, H.; Chabriat, J.P.; Grondin-Perez, B.; Tourrand, C.; Brau, J. Thermal building simulation and computer generation of nodal models. *Build. Environ.* **1996**, *31*, 207–214. [CrossRef]
17. Wetter, M. GenOpt-A generic optimization program. In Proceedings of the Seventh International IBPSA's Building Simulation Conference, Rio de Janeiro, Brazil, 13–15 August 2001.
18. Bigot, D.; Miranville, F.; Boyer, H.; Bojic, M.; Guichard, S.; Jean, A. Model optimization and validation with experimental data using the case study of a building equipped with photovoltaic panel on roof: Coupling of the building thermal simulation code ISOLAB with the generic optimization program GenOpt. *Energy Build.* **2013**, *58*, 333–347. [CrossRef]
19. *French Thermal Rules 2012*; Règles Th-U: Paris, France, 2012.
20. Guichard, S. *Contribution à l'étude des parois complexes intégrant des matériaux à changements de phase Modélisation, Expérimentation et évaluation de la performance thermique globale*; Université de La Réunion: Saint-Pierre, France, 2013. (In French)
21. Kuznik, F.; Virgone, J. Experimental investigation of wallboard containing phase change material: Data for validation of numerical modeling. *Energy Build.* **2009**, *41*, 561–570. [CrossRef]
22. David, D.; Kuznik, F.; Roux, J.-J. Numerical study of the influence of the convective heat transfer on the dynamical behaviour of a phase change material wall. *Appl. Therm. Eng.* **2011**, *31*, 3117–3124. [CrossRef]
23. Dutil, Y.; Rousse, D.R.; Salah, N.B.; Lassue, S.; Zalewski, L. A review on phase-change materials: Mathematical modeling and simulations. *Renew. Sustain. Energy Rev.* **2011**, *15*, 112–130. [CrossRef]
24. Guichard, S.; Miranville, F.; Boyer, H.; La Réunion, F. A Mathematical Model of Phase Change Materials (PCM) used in Buildings. In Proceedings of the Third IASTED African Conference, Gaborone, Botswana, 6–8 September 2010.
25. Dauvergne, J.L. Réduction et inversion de problèmes de diffusion thermique avec changement de phase. Ph.D. Thesis, University of Bordeaux, Bordeaux, France, 2008. (In French).
26. Miranville, F.; Lauret, P.; Medina, M.; Bigot, D. A simplified model for radiative transfer in building enclosures with low emissivity walls: Development and application to radiant barrier insulation. *J. Solar Energy Eng.* **2011**, *133*. [CrossRef]
27. Mara, T.A.; Boyer, H.; Garde, F. Parametric sensitivity analysis of a test cell thermal model using spectral analysis. *J. Solar Energy Eng.* **2002**, *124*, 237–242. [CrossRef]
28. Mara, T.A.; Garde, F.; Boyer, H.; Mamode, M. Empirical validation of the thermal model of a passive solar cell test. *Energy Build.* **2001**, *33*, 589–599. [CrossRef]
29. Lauret, A.J.P.; Mara, T.A.; Boyer, H.; Adelard, L.; Garde, F. A validation methodology aid for improving a thermal building model: Case of diffuse radiation accounting in a tropical climate. *Energy Build.* **2001**, *33*, 711–718. [CrossRef]
30. Bigot, D. *Contribution à l'étude du couplage énergétique enveloppe/système dans le cas de parois complexes photovoltaïques (pc-pv)*; Université de La Réunion: Le Tampon, France, 2011. (In French)
31. Alamdari, F.; Hammond, G.P. Improved data correlations for buoyancy-driven convection in rooms. *Build. Serv. Eng. Res. Technol.* **1983**, *4*, 106–112. [CrossRef]